On the Surface Lattice of Microtubules: Helix Starts, Protofilament Number, Seam, and Handedness

E.-M. Mandelkow,* R. Schultheiss,* R. Rapp,* M. Müller,‡ and E. Mandelkow*

*Max-Planck-Institut für medizinische Forschung, Abteilung Biophysik, D-6900 Heidelberg, Federal Republic of Germany; ‡ETH Zürich, Abteilung für Zellbiologie und Elektronenmikroskopie, CH-8092 Zürich, Switzerland. R. Schultheiss's present address is Dornier Medizintechnik GmbH, D-8034 Germering, Federal Republic of Germany. R. Rapp's present address is IBM, D-7030 Böblingen, Federal Republic of Germany. E.-M. and E. Mandelkow's present address is Max-Planck-Arbeitsgruppe für strukturelle Molekularbiologie, D-2000 Hamburg 52, Federal Republic of Germany.

Abstract. The tubulin monomers of brain microtubules reassembled in vitro are arranged on a 3-start helix, irrespective of whether the number of protofilaments is 13 or 14. The dimer packing is that of the B-lattice described for flagellar microtubules. This implies that the tubulin core of microtubules contains at least one helical discontinuity. Neither 5-start nor 8-start helices have a physical significance and thus cannot be implicated in models of microtubule elongation, but the structure is compatible with elongation of protofilaments by dimers or protofilamentous oligomers.

The inner and outer surfaces of the microtubule wall can be visualized by propane jet freezing, freeze fracturing, and metal replication, at a resolution of at least 4 nm. The 3-start helix is left-handed, in contrast to a previous study based on negative staining and shadowing. The reasons for this discrepancy are discussed.

When flagellar outer doublet microtubules were studied by image reconstruction, it was found that both A- and B-tubules had the same arrangement of monomers but a different dimer lattice (1). Both had longitudinal protofilaments with a 4-nm repeat of monomers, and adjacent protofilaments were staggered by ~0.9 nm, thus generating a 3-start helix of monomers. When this helix was followed, it was found that the A- or B-tubulin molecules could either alternate (α-β-α-$\beta\cdots$, A-lattice) or be aligned (α-α-$\alpha\cdots$ or β-β-$\beta\cdots$, B-lattice). With 13 protofilaments, the A-lattice could be helically symmetric, whereas the B-lattice could not. Since the flagellar B-tubule is not a closed cylinder, the potential lack of symmetry did not present a conceptual problem.

This situation changed when cytoplasmic microtubules became available for structural investigation. All evidence accumulated thus far indicates that they have a B-type dimer lattice. These studies include x-ray fiber diffraction of oriented microtubules (23) as well as optical diffraction and image reconstruction of polymorphic forms observed concomitant with microtubule assembly (hoops [24], sheets [10, 34], and microtubules [28]). This means that cytoplasmic microtubules lack helical symmetry. Recently similar conclusions have been reported for flagellar central pair microtubules and tubules repolymerized from B-tubulin (21, 22).

The B-lattice with its lack of symmetry implies that the 5-start and 8-start helices of dimers postulated for flagellar A-tubules have no physical significance. This has a bearing not only on structural models of microtubules (which until now are mostly represented in a symmetrical fashion in reviews and text books, despite evidence to the contrary), but also for models of assembly that tend to assume helical symmetry (e.g., reference 9).

The problem of lattice discontinuity would disappear if microtubules reassembled in vitro had a different number of helix starts and protofilaments (e.g., 4/14 instead of 3/13). Several authors have indeed shown that reassembled microtubules frequently have 14 protofilaments (19, 32). We have therefore re-investigated the structure of microtubule walls under conditions in which microtubules reassembled with either 13 or 14 protofilaments. In both cases we find a combination of 3-start helix and B-lattice, which means that the discontinuity of the microtubule lattice is an intrinsic feature of tubulin assembly. This excludes helical assembly models but is compatible with models based on lateral protofilament association and protofilament elongation.

A second question we address here is the helix handedness of microtubules. Conflicting images have been presented in the literature, based on different experimental techniques. We have now approached the problem by the propane jet freezing method developed by Müller et al. (30), followed by metal replication. It combines the advantages of high resolution and reproducible interpretability. We conclude that the 3-start helix is left-handed, in agreement with earlier results obtained from image processing (1, 8, 12), but in contrast to previous results from negative staining and shadowing (34) or cryo-block freezing (16).

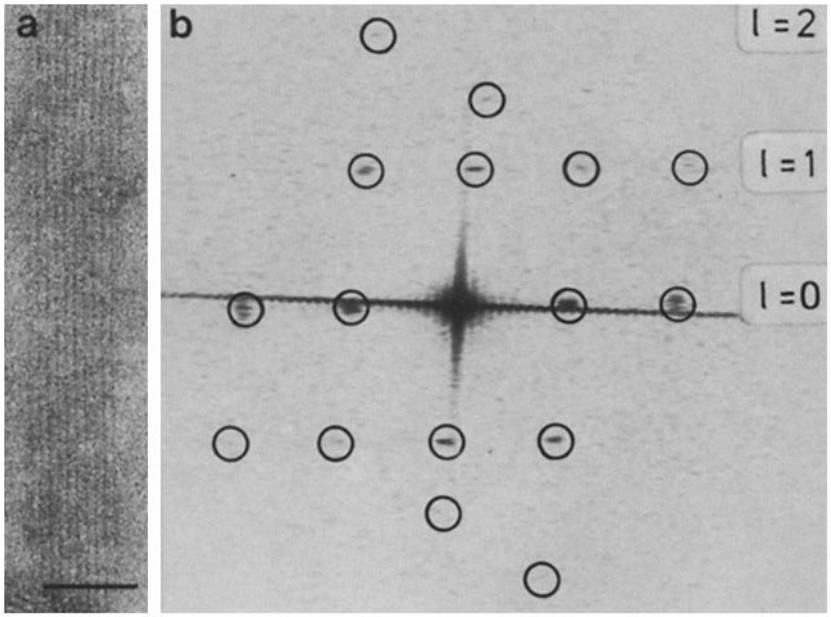

Figure 1. Electron micrograph of sheet and its optical diffraction pattern. (*a*) Sheet (assembled in 0.1 M MES, pH 6.6, with 25% glycerol), with longitudinal striations due to protofilaments and shallow cross-striations going up and to the left. Note main periodicity of 4-nm and the fainter striations of 8-nm periodicity. (*b*) Optical diffraction pattern. The main layer lines correspond to order of 4 nm (l = 0,1,2). The 8-nm periodicity is most pronounced midway between layer lines 1 and 2 (3rd order of 8 nm). The position of the reflection indicates a B-lattice. Bar, 0.05 μm.

Materials and Methods

Protein Preparation

Microtubule protein was prepared by one of the temperature cycle methods (5, 35). The usual reassembly buffers are either 0.1 M 2-(*N*-morpholino)ethane sulfonic acid (MES)[1] pH 6.6 or 0.1 M Pipes pH 6.9 or 6.6, with or without 25% glycerol. The buffer type, pH value, and nucleation conditions are known to affect the curvature of the microtubule wall and the number of protofilaments resulting from it (6, 17). In our conditions of protein preparation and assembly we find 13-protofilament microtubules (>90%) with 0.1 M MES, pH 6.6, and 25% glycerol, in agreement with earlier results (23). With 0.1 M Pipes, pH 6.9 or 6.6, with or without glycerol we obtain 14-protofilament microtubules, confirming the observations of Scheele et al. (32). The main effect of glycerol is to increase the fraction of incomplete microtubule walls during the early stage of assembly. In thin sections these appear as C-tubules. In negative stain they are usually flattened into sheets containing a single layer of protofilaments; this allows an accurate determination of lattice parameters (12).

Electron Microscopy and Image Interpretation

Twice cycled microtubule protein was resuspended at 2–3 mg/ml in the reassembly buffer appropriate for 13 or 14 protofilaments (with 25% glycerol), polymerized for 5 min, placed on carbon-coated grids, and observed by negative-stain electron microscopy (1% uranyl acetate or formate) in a Philips EM400T microscope (Philips Nederland B.V., Eindhoven, Netherlands). Images of sheets were selected by the sharpness of their optical diffraction patterns and photographed on 35-mm film using a diffractometer with an f = 100 cm lens.

Lattice constants were obtained either from photographic enlargements of optical diffraction patterns or on a microdensitometer (Nikon Inc., Garden City, NY). Three parameters were recorded: (*a*) the distance R of the [1,0] reflection on the equator (the inverse of which is proportional to the separation of protofilaments), (*b*) the distance Z of the first layer line (giving the axial repeat of tubulin monomers), and (*c*) the angle γ between the line connecting the origin and the [0,1] reflection and the meridian (equal to the inclination of the cross-striations that correspond to the 3-start helix). The axial stagger between adjacent protofilaments is then $S = (Z/R)\tan\gamma \cdot 4$ nm. Note that S is internally calibrated and therefore independent of magnification. For each assembly condition (giving 13 or 14 protofilaments per microtobule), the data from the sharpest diffraction patterns were plotted on a histogram from which the mean shift per protofilament and the standard deviation were calculated.

The number of protofilaments per microtubule was determined from thin sections of tannic acid–stained samples (36).

[1] *Abbreviation used in this paper:* MES, 2-(*N*-morpholino)ethane sulfonic acid.

Propane Jet Freezing and Metal Replication

Microtubule solutions were frozen rapidly by a propane jet cooled at liquid nitrogen temperature (QFD 020, Balzers AG, Balzers, Liechtenstein; see reference 30). A droplet of the solution was applied to a 400-mesh gold grid, pressed flat between two copper disks, inserted into the apparatus, and quickly frozen and stored in liquid nitrogen until further processing. The samples were freeze-fractured by separating the copper disks in a Balzers BAF 301 unit (etching at −100°C, 2.5 min, 10^{-6} hPa) and rotary shadowed with 2-nm platinum at an angle of 25° and 20-nm carbon at 90°. The gold grid was then mounted in the microscope specimen holder with the shadowed side up. The method has three advantages: The thin layer of solution ensures high freezing rates of the whole sample, the attachment to the gold grid allows unambiguous orientation of the replica (this is critical for determining the helix hand), and the removal of the protein from the replica is unnecessary.

Alternatively, samples were frozen by the cryo-block method, i.e., by dropping them onto a liquid helium–cooled copper block (Cryoblock, Reichert-Jung GmbH, Nussloch, FRG; see Escaig [13]). This procedure achieves somewhat higher freezing rates that are however not critical in the case of solutions. The disadvantages are the higher cost (liquid helium) and the necessity to dissolve the protein from the replica, which introduces uncertainties in the orientation of the replica. The propane jet method was therefore preferred.

Results

Protofilament Number, Helix Starts, and Seam

In analyzing the surface lattice, we concentrated on opened-up microtubule walls since they allow the most accurate measurement of the axial shift between protofilaments. By contrast, microtubules are usually somewhat distorted and their front and back surfaces overlap in projection; both factors complicate the analysis (28). Fig. 1 shows a sheet and its optical diffraction pattern with main layer lines up to 2-nm resolution. The position of the reflections confirms that the monomer lattice is that of microtubules (10, 12, 34). The reflections from the dimer lattice are always very weak since the difference between A- and B-tubulin is small. In the example of Fig. 1 there is a clear reflection midway between the [0,1] and [0,2] reflections, at an axial resolution of 8 nm/3 = 2.7 nm. This identifies the lattice as that of B-tubules (1). Corresponding reflections midway between the origin and the [0,1] reflection are also sometimes seen. They are generally weak with sheets, probably because of their radiation sensitiv-

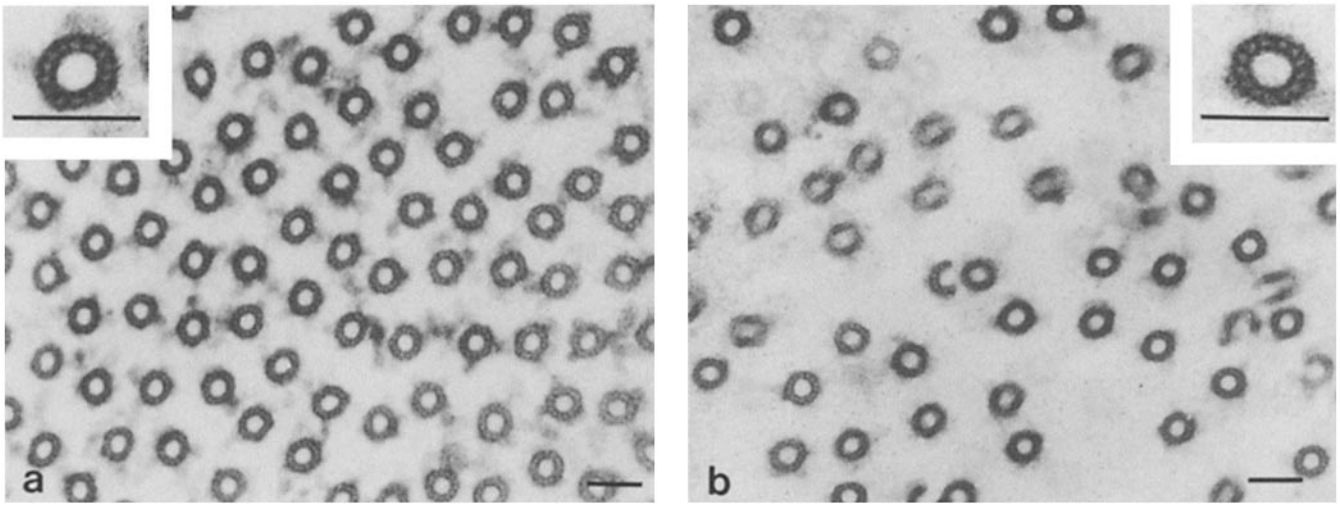

Figure 2. Sections showing microtubules with (*a*) 14 and (*b*) 13 protofilaments. Microtubule protein was polymerized for 20 min in (*a*) 0.1 M Pipes reassembly buffer at pH 6.9, or (*b*) 0.1 M MES reassembly buffer at pH 6.6, with 25% glycerol, then pelleted, fixed in 1% tannic acid, 1% glutaraldehyde, and processed for sectioning as described (25). Bars, 0.05 μm.

ity (3), but they are more pronounced with larger arrays such as hoops (24). We did not observe any reflections corresponding to the A-lattice. These findings agree with x-ray patterns of microtubules whose layer lines at odd orders of 8 nm are also dominated by the B-lattice (23).

Since the B-lattice would imply some discontinuity in the microtubule surface lattice, we asked whether symmetry could be achieved by changes in protofilament number and stagger. Fig. 2 shows thin sections of microtubules containing, homogeneously, either 13 or 14 protofilaments. The axial shift per protofilament found in these conditions is illustrated in Fig. 3. For a 3-start helix one expects a shift of 12 nm/k, where k is the number of protofilaments (is 0.923 nm for 13 protofilaments, 0.857 nm for 14 protofilaments). For a 4-start helix the shift would be 16 nm/k (is 1.231 nm for 13, 1.143 nm for 14 protofilaments). The histograms are centered around 0.89 and 0.79 nm, with standard deviations ~0.18 nm. Both distributions are compatible with a 3-start helix, but not with a 4-start helix. Thus the intersubunit interactions are nearly identical in the two conditions, and the variable number of protofilaments is accounted for by minor changes in wall curvature. The combination of B-lattice and 3-start helix implies that there must be a discontinuity or seam in the surface lattice which to a first approximation is independent of the protofilament number (see models *1* and *2* of Fig. 4, top).

We then asked if a seam in the microtubule wall could be visualized directly. In principle this would require a positive identification of α- and β-tubulin molecules at high resolution. This is not possible with negatively stained specimens, given the low contrast between the two tubulins (imagine Fig. 4 with the contrast between black and white reduced to an almost uniform grey). However, there are several types of observations indicating that there are special seam-like interactions between particular pairs of protofilaments. One is that the protofilaments forming junctions between microtubule walls are unusually tightly packed (down to 3.5 nm, compared with the usual 5 nm). They can be found in S-shaped hooks, hoops, and other composite assembly forms (not shown; see Fig. 2 of reference 25, or Fig. 6 of reference 26). Secondly,

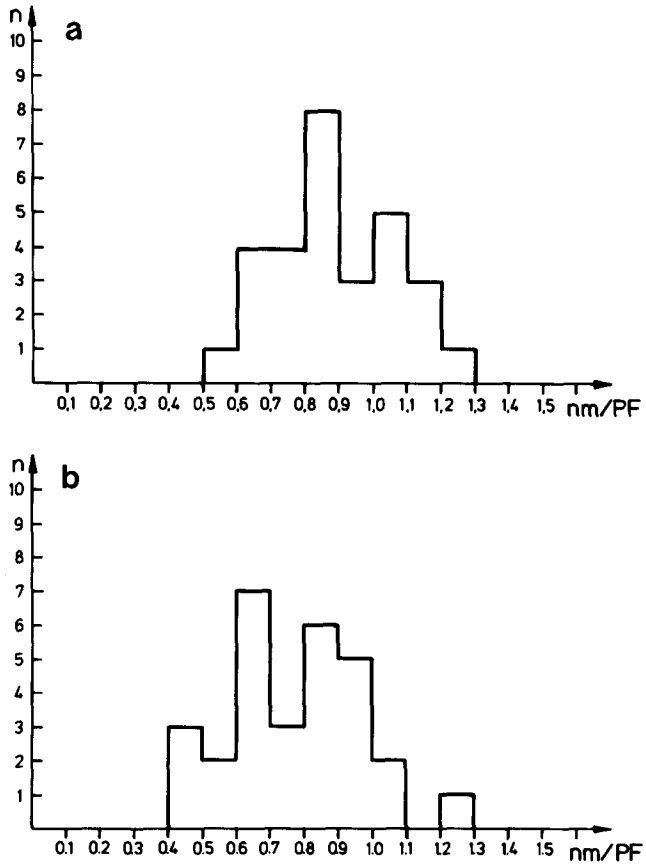

Figure 3. Histograms showing inclination of cross-striations of sheets prepared in different conditions. (*a*) 0.1 M Pipes pH 6.6, 25% glycerol (favoring 14 protofilaments) and (*b*) 0.1 M MES pH 6.6, 25% glycerol (favoring 13 protofilaments). The y-axis shows the number of particles, the x-axis shows the stagger between adjacent protofilaments. In *a* the mean shift per protofilament is 0.89 nm (SD 0.17 nm, 33 particles); in *b* the mean shift is 0.79 nm (SD 0.19, 32 particles).

freeze-fractured microtubules are sometimes seen to be split over short distances at several points along their length, with the split occurring between the same pair of protofilaments.

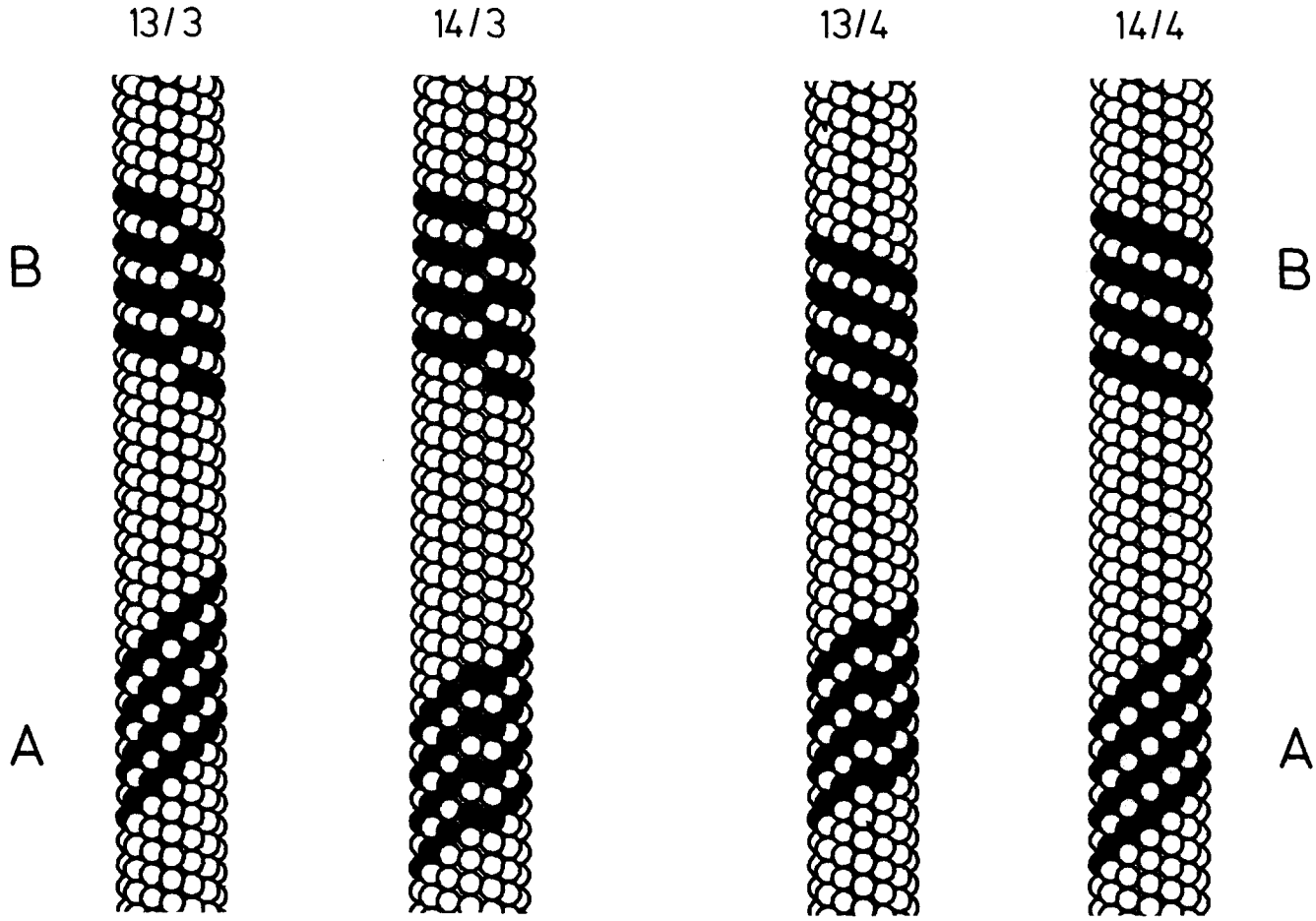

Figure 4. Models of lattices for the various combinations of protofilament number, helix starts, and dimer lattices. Each tubulin monomer is represented by a sphere (black = α, empty = β, axial separation of monomers is 4 nm). The two models on the left are built from 3-start helices of monomers and 13 or 14 protofilaments (13/3 and 14/3). The two models on the right are based on 4-start helices (13/4 and 14/4, not observed in practice). The A-lattice is shown in the lower part, the B-lattice in the upper part of the models. The discontinuity, when present, is between the two central protofilaments. Note that a combination of 3-start helix and B-lattice is always discontinuous (models *1* and *2*, top), and that the A-lattice is continuous in the case of 13/3 (model *1*) but discontinuous in the case of 14/3 (model *2*).

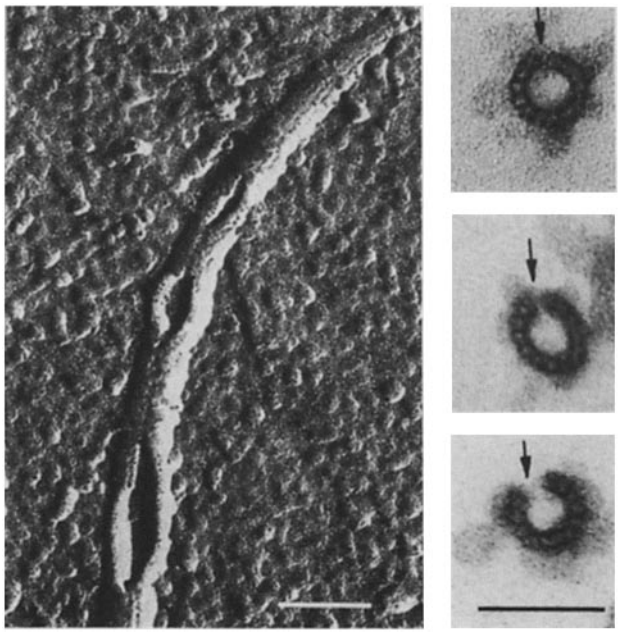

Figure 5. Microtubule walls showing structural analogues of a discontinuity. (*Left*) Microtubule rapidly frozen by the propane jet method, freeze-fractured, and replicated by platinum/carbon shadowing. Note splitting of microtubule wall between the same pair of protofilaments along the whole length. (*Right*) Microtubule protein polymerized briefly (2 min) in 0.1 M Pipes reassembly buffer pH 6.9, fixed for 10 min by 1% tannic acid, 1% glutaraldehyde in reassembly buffer at 37°C, pelleted and processed for thin sectioning as above. At early stages of assembly there is an increased number of incompletely closed microtubule walls with variable gaps, suggesting that assembly is non-helical and that a special interaction between protofilaments is necessary for closure. Bars, 0.05 μm.

This suggests a seam whose stability is lower than that of the bonds between the other protofilaments (Fig. 5, *left*). Finally, the well-known occurrence of C-shaped incomplete microtubule walls is a strong argument for the non-helical growth of microtubules and the requirement for closure between a special pair of protofilaments (Fig. 5, *right*).

Helix Hand of Jet-Frozen and Fractured Microtubules

When a microtubule solution is frozen rapidly by a cold propane jet, fractured, lightly etched, and replicated by metal shadowing, one can observe different appearances depending on the position of a microtubule relative to the fracture plane (Fig. 6): (*a*) When the outer surface of a microtubule is exposed one can distinguish the longitudinal protofilaments, but the subunits are distorted so that other helical lines are

blurred. In particular, the inclination of the 3-start helix cannot be identified reliably. (*b*) When the microtubule is fractured open the inside of the back wall becomes visible. It is dominated by oblique lines running up and to the right at an angle of ~13–15°, and with an axial separation of 4 nm. Thus they correspond to the 3-start helix of tubulin monomers. The inclination means that this helix is left-handed.

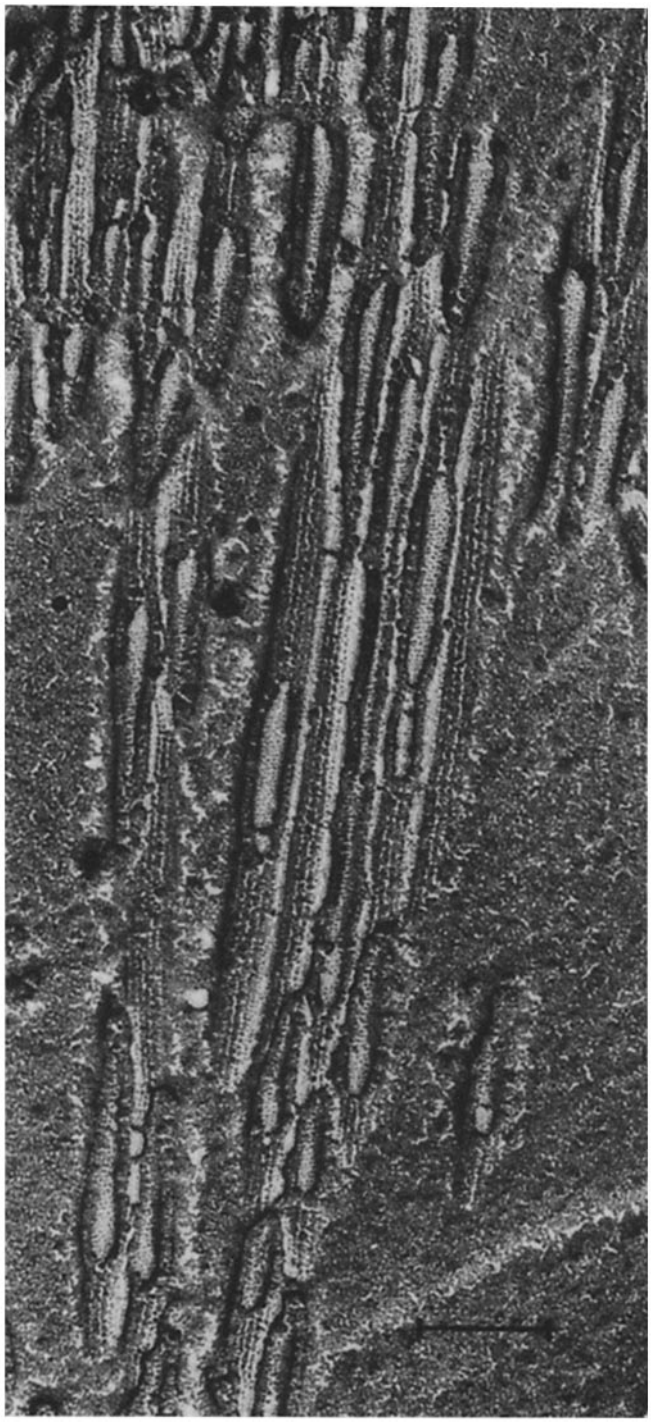

Figure 6. Microtubules quickly frozen on a gold grid by the propane jet method, freeze-fractured, and rotary shadowed with platinum. The outside surfaces show longitudinal protofilaments, the insides show oblique lines running up and to the right corresponding to the left-handed 3-start helix. The resolution is at least 4 nm (axial separation of helical lines). Bar, 0.1 μm.

The longitudinal protofilaments are usually not visible on the inside.

Quick freezing by the cryo-block method yields similar images (not shown). However, the inclinations of the helical lines on the inside surfaces may be up and to the left or to the right. This is explained by the fact that parts or all of the replica may be inverted when it is transferred to the grid. Thus the method is less reliable for determining the absolute helix hand. This may be the reason for the apparent differences in published images obtained by the cryo-block method (compare references 16 and 18).

The results from propane-jet freezing contradict our earlier conclusions about the helix hand, using a combination of negative staining and metal shadowing and the same conventions of electron imaging and printing (34). In that study we investigated long incomplete microtubule walls (sheets) which retained a microtubule-like wall curvature. These samples showed an apparently right-handed helix (oblique striations up and to the left when viewing at the inside surface). However, the opposite curvature was also sometimes observed, although it was maintained only over short stretches and therefore considered an artifact (compare the two particles in Fig. 1 *d* of reference 34). It therefore appears that the curvatures of negatively stained opened-up microtubule walls may either be right-side-out (reproducing the correct helix hand) or inside-out (generating the opposite hand), presumably depending on their rigidity and the forces that act on them during adsorption, staining, and drying.

Discussion

The Lattice Discontinuity

Several theoretical combinations of protofilament numbers, helix starts, and lattice types are illustrated in Fig. 4, and Table I shows whether the lattices are symmetric or not. In our experiments, only the combination of 3-start helix and B-lattice was observed. This is illustrated in Fig. 7. The findings have consequences for models of microtubule structure as well as assembly. The combination of a 3-start helix and a B-lattice implies that there is a discontinuity somewhere in the microtubule wall. In every turn of the 3-start helix the sequence of like subunits (either α-α-$\alpha\cdots$ or β-β-$\beta\cdots$) must be interrupted at least once by an α-β bond. The discontinuity

Table I. Relationship of Protofilament Number, Number of Helix Starts, and Microtubule Symmetry for the A- and B-Lattices

	A-lattice	B-lattice
13 Pf		
3-Start	Sym	Asym
4-Start	Asym	Sym
14Pf		
3-Start	Asym	Asym
4-Start	Sym	Sym

The A-lattice is symmetric when the protofilament (Pf) number and helix starts are both either even or odd (13/3 or 14/4). The B-lattice is symmetric only with an even number of helix starts, independent of protofilament number (13/4 or 14/4). The observed combinations (13/3 or 14/3) and the observed B-lattice show that microtubules must contain at least one discontinuity. Even if an A-lattice existed it would be discontinuous with 14 protofilaments and a 3-start helix. Sym, symmetric. Asym, asymmetric.

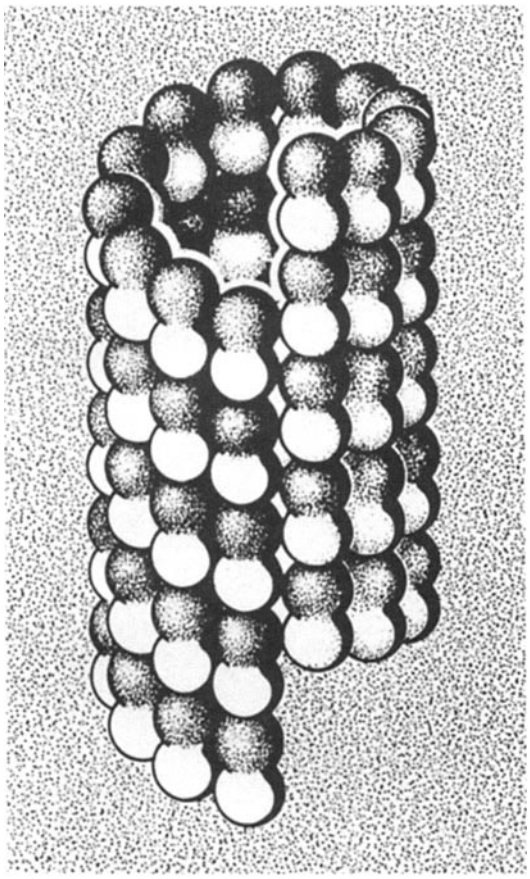

Figure 7. Model summarizing the key features of a microtubule lattice with 13 protofilaments, 3-start helix, and a B-lattice. Note helical discontinuity.

could be confined to two adjacent protofilaments, as shown in Fig. 5, and as suggested by the special interactions and stabilities between certain pairs of protofilaments (termed junctions in previous studies [25, 26]). However, the possibility that the discontinuities are distributed over the microtubule wall cannot be excluded. The function of a seam is unknown at present. One possibility is that it helps to close the microtubule wall when it is nucleated by lateral association of protofilamentous oligomers. It could also define the potential attachment site of some microtubule-associated proteins and/or the attachment site of another microtubule wall (forming hooks or doublet tubules in appropriate assembly conditions [25]). Thirdly, a discontinuity could be required as a nucleation site for the longitudinal and/or lateral growth of a microtubule wall (or two associated walls). In any case, the energy difference between the lateral bonds of like and unlike monomers (i.e., α-α or β-β vs. α-β) need not be large, considering the homologies between the two monomers.

The lattice of tubulin subunits has an influence on possible lattices of microtubule-associated proteins. Their variable stoichiometry (19) and the absence of well-defined diffraction spots suggests that they are normally not periodic. However, it is possible to define a periodic arrangement of microtubule-associated proteins based on the assumption that the underlying tubulin core has an A-lattice (2). Such models would have to be adapted to the B-lattice, and they would have to include a discontinuity as well.

The B-lattice simplifies models of elongation. Each end can in principle be rather smooth since the shift between the terminal subunits is small, apart from a step at the discontinuity (Fig. 7). This would allow the simultaneous addition of several mutually independent subunits. By contrast, with the A-lattice the protofilaments would terminate at different levels so that one has to postulate different probabilities of subunit addition (37). In particular, the B-lattice lends itself to elongation of protofilaments by dimers or short protofilamentous oligomers (4). However, it is not compatible with models based on elongation along the 5-start or 8-start helices since these have no physical significance.

Protein assemblies are usually made from subunits having both (relatively) constant bonds as well as more flexible ones. In the case of tubulin the axial bond is the most invariant one; it defines the dimer, the oligomer, and the protofilament. In normal assembly conditions the lateral bonds between adjacent protofilaments are also fairly reproducible; they define the B-lattice. By contrast, when oligomers associate during nucleation the curvature of the incipient microtubule wall is rather ill-defined, resulting in a variable number of protofilaments per tubule. In the case of spontaneous assembly this seems to depend mainly on buffer conditions and on local charge densities. For example, the curvature of the wall decreases at low pH or in high concentrations of Pipes (6, 17). With seeded assembly, the microtubule is simply propagated with the curvature determined by the seed (14, 32). In either case, the wall curvature and the protofilament number resulting from it are of secondary importance, compared with the primary interactions along a protofilament (4-nm monomer repeat) and between two adjacent ones (mostly B-lattice interaction, ~0.9-nm stagger). Strictly speaking the results presented here refer to microtubules re-assembled in vitro, and one could ask if they are applicable to cellular microtubules as well. We think this is justified, for the reason that on the level of monomers, the nearest-neighbor interactions in native and re-assembled microtubules are the same (compare, for example, references 1 and 22), and there is no evidence to suggest that the dimer lattices should be different. Judging by other macromolecular assemblies, any differences in bonding are likely to be restricted to the level of quasiequivalent conformational changes (7).

The Helix Hand

When searching the literature for evidence of the microtubule helix hand one finds examples for both right- and left-handedness. The problem of determining the hand is conceptually simple: one only has to identify the front or back surface of the particle and measure the inclination of the helix lines on it. Ambiguities arise from the fact that a helical structure made up of subunits contains a variety of left- and right-handed helices; their contrast varies and depends on methods of staining or replication; and negative staining does not normally allow a firm distinction between front and back. A priori surface replication would appear as the most reliable method, but even here published evidence is ambiguous (e.g., right-handed, references 16 and 29; left-handed, reference 18, and this report). The problem is that even when conventions of imaging are carefully kept a change in orientation can occur during preparation of the replica. This ambiguity is largely (but not totally) overcome by the jet freezing procedure, in which the orientation of the sample is fixed relative

to the gold grid support. The results support a left-handed 3-start helix (implying a right-handed 10-start helix, etc.).

This result agrees with earlier studies based on negatively stained flagellar microtubules (8, 20) or sheets of brain tubulin (12). By contrast, our previous studies with negatively stained and metal shadowed tubulin sheets indicated right-handedness (34). In hindsight, comparison of the data reveals another source of ambiguity: Curved sheets can be right-side-out or inside-out. In our earlier conditions of preparation the inside-out particles appeared rather homogeneous and therefore more believable, whereas the true curvature (judging by the jet freezing results) was preserved only over short stretches.

We have also obtained images of frozen microtubules similar to Fig. 6 using the liquid helium cooled cryo-block apparatus developed by Escaig (13), the design of which is similar to that of Heuser et al. (15). The jet freezing results indicate that sufficiently high freezing rates can be achieved even at liquid nitrogen temperatures, particularly in the case of solutions that can be made arbitrarily thin (as reviewed in reference 31). Possible differences in preservation between the two methods appear to be below the limit of resolution imposed by the subsequent processing. Similarly, differences in contrast may be explained by the extent of etching (deep or shallow) rather than the method of freezing (compare references 16 and 33). Thus the lower cost and simplicity of jet freezing may make this the preferred method for freeze fracture of solutions. Finally we note that microtubule solutions can even be vitrified by blotting them into a thin layer on a grid (11) and dipping it into cryogen; this method is suitable for the observation of frozen-hydrated microtubules in a cryo-electron microscope (27).

We would like to thank U. Rühl for excellent technical assistance, Dr. D. Schroeter and Dr. B. Agostinini for making their freeze fracture apparatus available, A. Lahm for the drawing of Fig. 4, and K. H. Söhnholz for Fig. 7.

This work was supported in part by the Deutsche Forschungsgemeinschaft.

Received for publication 3 April 1985, and in revised form 6 November 1985.

References

1. Amos, L. A., and A. Klug. 1974. Arrangement of subunits in flagellar microtubules. *J. Cell Sci.* 14:523–549.

2. Amos, L. A. 1977. Arrangement of high molecular weight associated proteins on purified mammalian brain microtubules. *J. Cell Biol.* 72:642–654.

3. Baker, T. S. and L. A. Amos. 1978. Structure of tubulin dimer in zinc-induced sheets. *J. Mol. Biol.* 123:89–106.

4. Bordas, J., E.-M. Mandelkow, and E. Mandelkow. 1983. Stages of tubulin assembly and disassembly studied by time-resolved synchrotron X-ray scattering. *J. Mol. Biol.* 164:89–135.

5. Borisy, G. G., J. M. Marcum, J. B. Olmsted, D. B. Murphy, and K. H. Johnson. 1975. Purification of tubulin and associated high molecular weight proteins from porcine brain and characterization of microtubule assembly in vitro. *Ann. NY Acad. Sci.* 253:107–132.

6. Burton, P. R., and R. H. Himes. 1978. Electron microscope studies of pH effects on assembly of tubulin free of associated proteins: delineation of substructure by tannic acid staining. *J. Cell Biol.* 77:120–133.

7. Caspar, D. L. D., and A. Klug. 1962. Physical principles in the construction of regular viruses. *Cold Spring Harbor Symp. Quant. Biol.* 27:1–24.

8. Chasey, D. 1974. Left-handed subunit helix in flagellar microtubules. *Nature (Lond.).* 248:611–612.

9. Chen, Y., and T. L. Hill. 1985. Monte Carlo study of the GTP cap in a five-start helix model of a microtubule. *Proc. Natl. Acad. Sci. USA.* 82:1131–1135.

10. Crepeau, R. H., B. McEwen, and S. J. Edelstein. 1978. Differences in alpha and beta polypeptide chains of tubulin resolved by electron microscopy with image reconstruction. *Proc. Natl. Acad. Sci. USA.* 75: 5006–5010.

11. Dubochet, J., J. Lepault, R. Freeman, J. Berriman, and J.-C. Homo. 1982. Electron microscopy of frozen water and aqueous solutions. *J. Microsc.* 128:219–237.

12. Erickson, H. P. 1974. Microtubule surface lattice and subunit structure and observations on reassembly. *J. Cell. Biol.* 60:153–167.

13. Escaig, J. 1982. New instruments which facilitate rapid freezing at 83 K and 6 K. *J. Microsc.* 126:221–229.

14. Evans, L., T. Mitchison, and M. Kirschner. 1985. Influence of the centrosome on the structure of nucleated microtubules. *J. Cell Biol.* 100:1185–1191.

15. Heuser, J. E., T. S. Reese, M. J. Dennis, Y. Jan, L. Jan, and L. Evans. 1979. Synaptic vesicle exocytosis captures by quick freezing and correlated with quantal transmitter release. *J. Cell Biol.* 81:275–300.

16. Heuser, J. E., and M. W. Kirschner. 1980. Filament organisation revealed in platinum replicas of freeze-dried cytoskeletons. *J. Cell Biol.* 86:212–234.

17. Himes, R. H., P. R. Burton, and J. M. Gaito. 1977. Dimethyl sulfoxide-induced self-assembly of tubulin lacking associated proteins. *J. Biol. Chem.* 252:6222–6228.

18. Hirokawa, N. 1982. Cross-linker system between neurofilaments, microtubules, and membranous organelles in frog axons revealed by the quick-freeze, deep-etching method. *J. Cell Biol.* 94:129–142.

19. Kim, H., L. I. Binder, and J. L. Rosenbaum. 1979. The periodic association of MAP2 with brain microtubules in vitro. *J. Cell Biol.* 80:266–276.

20. Linck, R. W., and L. A. Amos. 1974. The hands of helical lattices in flagellar doublet microtubules. *J. Cell Sci.* 14:551–559.

21. Linck, R. W., G. E. Olson, and G. L. Langevin. 1981. Arrangement of tubulin subunits and microtubule-associated proteins in the central-pair microtubule apparatus of squid sperm flagella. *J. Cell Biol.* 89:309–322.

22. Linck, R. W., and G. L. Langevin. 1981. Reassembly of flagellar B(alpha-beta) tubulin into singlet microtubules: consequences for cytoplasmic microtubule structure and assembly. *J. Cell Biol.* 89:323–337.

23. Mandelkow, E., J. Thomas, and C. Cohen. 1977. Microtubule structure at low resolution by X-ray diffraction. *Proc. Natl. Acad. Sci. USA.* 74:3370–3374.

24. Mandelkow, E.-M., E. Mandelkow, P. N. T. Unwin, and C. Cohen. 1977. Tubulin hoops. *Nature (Lond.).* 265:655–657.

25. Mandelkow, E.-M., and E. Mandelkow. 1979. Junctions between microtubule walls. *J. Mol. Biol.* 129:135–148.

26. Mandelkow, E., R. Schultheiss, and E.-M. Mandelkow. 1984. Assembly and three-dimensional image reconstruction of tubulin hoops. *J. Mol. Biol.* 177:507–529.

27. Mandelkow, E.-M., and E. Mandelkow. 1985. Unstained microtubules studied by cryo-electron microscopy: substructure, supertwist, and disassembly. *J. Mol. Biol.* 181:123–135.

28. McEwen, B., and S. Edelstein. 1980. Evidence for a mixed lattice in microtubules reassembled in vitro. *J. Mol. Biol.* 139:123–145.

29. Moor, H. 1966. Der Feinbau der Mikrotubuli in Hefe nach Gefrierätzung. *Protoplasma.* 64:89–103.

30. Müller, M., N. Meister, and H. Moor. 1980. Freezing in a propane jet and its application in freeze-fracturing. *Mikroskopie.* 36:129–140.

31. Plattner, H., and L. Bachmann. 1982. Cryofixation: a tool in biological ultrastructural research. *Int. Rev. Cytol.* 79:237–304.

32. Scheele, R. B., L. G. Bergen, and G. G. Borisy. 1982. Control of the structural fidelity of microtubules by initiation sites. *J. Mol. Biol.* 154:485–500.

33. Schnapp, B. J., and T. S. Reese. 1982. Cytoplasmic structure in rapid-frozen axons. *J. Cell Biol.* 94:667–679.

34. Schultheiss, R., and E. Mandelkow. 1983. Three-dimensional reconstruction of tubulin sheets and re-investigation of microtubule surface lattice. *J. Mol. Biol.* 170:471–496.

35. Shelanski, M. L., F. Gaskin, and C. R. Cantor. 1973. Microtubule assembly in the absence of added nucleotides. *Proc. Natl. Acad. Sci. USA.* 70:765–768.

36. Tilney, L. G., J. Bryan, D. J. Bush, K. Fujiwara, M. S. Mooseker, D. B. Murphy, and D. H. Snyder. 1973. Microtubules: evidence for 13 protofilaments. *J. Cell Biol.* 59:267–275.

37. Weisenberg, R. C. 1980. Role of co-operative interactions, microtubule-associated proteins and guanosine triphosphate in microtubule assembly: a model. *J. Mol. Biol.* 139:660–677.